

Supporting Information

Green Synthesis of Catalytic Gold/Bismuth Oxyiodide Nanocomposites with Oxygen Vacancies for Treatment of Bacterial Infections

Chia-Lun Hsu,^{‡a} Yu-Jia Li,^{‡b} Hong-Jyuan Jian,^b Scott G. Harroun,^c Shih-Chun Wei,^a Rini Ravindranath,^a Jui-Yang Lai,^{*b,d,e} Chih-Ching Huang^f and Huan-Tsung Chang^{*a,g}

^aDepartment of Chemistry, National Taiwan University, Taipei, 10617, Taiwan

^bInstitute of Biochemical and Biomedical Engineering, Chang Gung University, Taoyuan, 33302, Taiwan

^cDepartment of Chemistry, Université de Montréal, Montréal, Québec, H3C 3J7, Canada

^dDepartment of Ophthalmology, Chang Gung Memorial Hospital, Linkou, Taoyuan, 33305, Taiwan

^eDepartment of Materials Engineering, Ming Chi University of Technology, New Taipei City 24301, Taiwan

^fDepartment of Bioscience and Biotechnology, National Taiwan Ocean University, Keelung, 20224, Taiwan

^gDepartment of Chemistry, Chung Yuan Christian University, Chungli District, Taoyuan City, 32023, Taiwan

[‡]These authors contributed equally

Correspondence: Professor Jui-Yang Lai, Institute of Biochemical and Biomedical Engineering, Chang Gung University, 259 Wen-Hwa 1st Road, Taoyuan 33302, Taiwan; Tel.: 011-886-3-211-8800 ext. 3598; Fax: 011-886-3-211-8668; E-mail: jylai@mail.cgu.edu.tw; Professor Huan-Tsung Chang, Department of Chemistry, National Taiwan University, Taipei, 10617, Taiwan; Tel.: 011-886-2-3366-1171; Fax: 011-886-2-3366-1171; E-mail: changht@ntu.edu.tw

Experimental section:

Chemicals. Tetrachloroauric(III) acid trihydrate was purchased from Alfa Aesar (Ward Hill, MA, USA). Potassium iodide, bismuth nitrate pentahydrate, tris(hydroxymethyl)aminomethane (Tris), and the other metal salts used were purchased from Mallinckrodt Baker (Phillipsburg, NJ, USA). Hydrogen peroxide was purchased from SHOWA (Tokyo, Japan). Amplex Red (AR, 10-acetyl-3,7-dihydroxyphenoxazine) was purchased from Invitrogen (Carlsbad, CA, USA). Six stains of *E. coli*, *K. pneumoniae*, *S. enteritidis*, *S. aureus*, *B. subtilis* and MRSA were obtained from the Institute of Food Science (Hsinchu, Taiwan). Fetal bovine serum (FBS) and all cell culture media were purchased from Gibco BRL (Grand Island, NY, USA). Antibiotic–antimycotic, L-glutamine and nonessential amino acids (NEAA) were obtained from Biowest (Lewes, UK). Alamar Blue reagent was purchased from BioSource (Camarillo, CA, USA). The LIVE/DEAD® BacLight™ bacterial viability kit, BacLight membrane potential kit, and B-PER bacterial protein extraction reagent (bacteria lysis agent) were purchased from Molecular Probes (Thermo Fisher Scientific Inc., Eugene, OR, USA). Tris–borate (50 mM, pH 7.0) was adjusted with boric acid. Phosphate buffered saline (PBS; containing 137 mM NaCl, 5.0 mM KCl, 0.5 mM CaCl₂, 1.0 mM MgCl₂, 10 mM Na₂HPO₄, and 2.0 mM KH₂PO₄, pH 7.4) was used to mimic physiological conditions. Milli-Q ultrapure water (18.2 MΩ·cm; EMD Millipore, Billerica, MA, USA) was used in all experiments.

Characterization of Au/BiOI nanocomposites. Transmission electron microscopy (TEM) images of the Au/BiOI nanocomposites were obtained using a Tecnai 20 G2 S-Twin transmission electron microscope (Philips/FEI, Hillsboro, OR, USA). X-ray photoelectron spectroscopy (XPS) was performed using an ES-CALAB 250 spectrometer (VG Scientific, East Grinstead, UK) with Al K α X-ray radiation as the X-ray excitation source. Binding energies were corrected using the C 1s peak at 284.6 eV as the standard. Possible components of the Au/BiOI nanocomposites were analyzed using laser desorption/ionization time-of-flight ionization mass spectrometry (LDI-TOF MS). Mass spectrometry experiments were performed in the reflectron positive-ion mode with an AutoflexIII

LDI-TOF MS (BrukerDaltonics, Bremen, Germany). The samples were irradiated with a pulse laser (Nd:YAG, 355 nm, 100 Hz; pulse width: 6 ns). A total of 500 pulse laser shots were applied to accumulate signals from five MALDI target positions under a laser irradiation power density of $5 \times 10^4 \text{ W cm}^{-2}$. For determination of the concentrations of metal ions and iodide ions by inductively coupled plasma mass spectrometry (ICP-MS; Agilent 7700 Series, Agilent Technologies, Santa Clara, CA, USA), the Au/BiOI nanocomposites samples were prepared in 2% HNO_3 . Powder X-ray diffraction (PXRD) experiments of nanocomposites for the structure refinement were collected at Taiwan beamline SP12B1 at SPring-8 (National Synchrotron Radiation Research Center, Hsinchu, Taiwan). The X-ray source of SP12B1 is delivered from a bending magnet which provided the X-ray source covering the energy range from 8 to 25 KeV. The powder diffraction patterns were recorded by a CCD detector (Rayonix MS225, Evanston, IL, USA) with a pixel size of 78 μm . 2D diffraction patterns were converted to 1D profiles with cake-type integration by the GSAS-II program. The distance from the sample to the CCD detector is $\sim 150 \text{ mm}$, which provides the angular resolution of 0.021 degree in two theta. Powdered samples were loaded into a 0.5 mm capillary for uniform absorption and free rotation during data collection. X-ray exposure time was 30 s during data collection. The powder diffraction patterns were recorded at the wavelength of 0.68898 Å (18 KeV) and calibrated by using the Bragg peaks of the NIST LaB_6 standard. Brunauer-Emmett-Teller (BET) specific surface area of the BiOI nanosheets and Au_1/BiOI nanocomposites were determined by conducting N_2 adsorption/desorption experiment using an automated gas adsorption analyzer BELSORP 28SA (Bel-Japan-Inc, Japan).

Enzyme kinetic analysis. We studied the kinetics of the oxidase-like catalytic reaction in a black 96-well microplate. The AR substrates (0–10 μM) in 5.0 mM Tris-borate solution (180 μL , pH 7.0) were separately added to each well of a microtiter plate, and aliquots (20 μL) of BiOI nanosheets (200 $\mu\text{g mL}^{-1}$) or Au/BiOI nanocomposites (200 $\mu\text{g mL}^{-1}$) in 5.0 mM Tris-borate (pH 7) were then added to the wells. The reaction progress was monitored every 30 s for 2 h by recording the fluorescence of the reaction product, resorufin, at 585 nm with an excitation wavelength of 540 nm.

Bacterial growth and assays. *E. coli*, *K. pneumoniae*, *S. enteritidis*, *S. aureus*, and *B. subtilis*, and were grown separately in Luria Broth (LB) media and MRSA in Luria Broth (LB) media containing 1% penicillin. A single colony of each strain was lifted from the LB agar plates and inoculated in LB media (10 mL). The cultures were grown at 37 °C with shaking (200 rpm) until the absorbance at 600 nm (OD₆₀₀) reached 1.0 (optical path length: 1.0 cm). A portion of each cell mixture (1.0 mL) was centrifuged (RCF 3,000 g, 10 min, 25 °C) and washed twice with 5 mM sodium phosphate buffer (pH 7.4) prior to further use.

SEM and TEM Images for bacteria. The bacterial suspensions of *E. coli* ($\sim 10^9$ CFU mL⁻¹, 2.0 mL) were centrifuged (RCF 3500 g, 10 min, 25 °C) and washed twice with 5.0 mM sodium phosphate buffer solution (pH 7.4). Aliquots (50 μ L) of *E. coli* suspensions (1.0×10^9 CFU mL⁻¹) were incubated with the BiOI nanosheets (100 μ g mL⁻¹) or Au₁/BiOI nanocomposites (100 μ g mL⁻¹) in 5.0 mM sodium phosphate solution (pH 7.4) for 2 h, which were then purified [RCF 3500 g for 10 min and washed with 5.0 mM sodium phosphate solution (pH 7.4, 1.0 mL \times 3)] to remove the matrix. The cells were fixed to the membrane using 4% paraformaldehyde in 5 mM sodium phosphate buffer (pH 7.4, 1.0 mL) for 1 h. They were then washed three times with 5 mM sodium phosphate buffer (pH 7.4, 1.0 mL). The resulting bacteria were mounted onto SEM specimen stubs and vacuum drying and then coated with gold by sputtering. The samples were observed under a Hitachi S-4800 (JEOL, Tokyo, Japan) scanning electron microscope. The nanomaterials-treated and untreated bacterial cultures (1 mL each) were centrifuged at RCF of 3500 g for 5 min. The pellet was then fixed using 2.5% glutaraldehyde in 5 mM sodium phosphate buffer (pH 7.4). The TEM images of the specimens were then recorded.

Viability of bacteria treated with Au/BiOI nanocomposites. The bacterial suspensions of *E. coli* (1.0×10^8 CFU mL⁻¹) were treated with BiOI nanosheets (100 μ g mL⁻¹) or Au₁/BiOI nanocomposites (100 μ g mL⁻¹) in 5.0 mM sodium phosphate solution (pH 7.4) at 37 °C with orbital shaking for different time durations (10, 30 and 60 min). The mixtures (1.0 mL) were then

centrifuged (RCF 3,500 g, 10 min, 25 °C), and washed twice with PBS (pH 7.4, 1.0 mL × 3) for fluorescence measurement and quantification of live and dead bacteria. The bacteria viability was determined by a LIVE/DEAD® BacLight™ bacterial viability kit. Briefly, for each 1 mL of the bacterial suspension, 3 µL of the dye mixture (SYTO 9:PI = 1:1) was added, and the dye-suspension mixtures were incubated at room temperature (27 °C) for 15 min in the dark. The mixtures were then centrifuged (RCF 3,500 g, 10 min, 25 °C) and washed twice with PBS (pH 7.4; 1.0 mL × 3), then dropped onto the glass slide for fluorescence measurement. The live/dead ratios of bacteria untreated and treated with nanomaterials at different time points were calculated from the intensities of blue (excitation with blue light 460–480 nm) and red (excitation with green light 510–530 nm) fluorescence using an Olympus IX71 microscope (Tokyo, Japan).

Permeability of bacterium membrane. The bacterial suspensions of *E. coli* (1.0×10^9 CFU mL⁻¹) were treated with solutions of BiOI nanosheets (100 µg mL⁻¹) or Au/BiOI nanocomposites (100 µg mL⁻¹) in 5.0 mM sodium phosphate solution (pH 7.4, 1.0 mL) containing 1.0 mM MgCl₂ and 10 mM KCl at 37 °C with orbital shaking for 1 h. Untreated and B-PER lysed *E. coli* were used as negative and positive control, respectively. The samples were centrifuged at a RCF of 3,500 g for 10 min, then the supernatants were retrieved for use in the colorimetric assay. The supernatants were diluted ten-fold in PBS solution (950 µL), and then aliquots of (50 µL of 1.0 mM) ortho-nitrophenyl-β-D-galactopyranoside (ONPG) substrate were added to the supernatants, and allowed to react at room temperature for 2 h. Then, 200 µL of each sample was transferred into a 96 well flat bottom microplate, and the absorbance of the samples was measured using a monochromatic microplate spectrophotometer (Synergy 4) at 420 nm.

Membrane potential of bacteria. The bacterial membrane potentials were measured using a BacLight membrane potential kit. The bacterial suspensions of *E. coli* (1.0×10^8 CFU mL⁻¹) were untreated or treated with BiOI nanosheets (20 µg mL⁻¹) or Au/BiOI nanocomposites (20 µg mL⁻¹) in 5.0 mM sodium phosphate solution (pH 7.4, 1 mL) at 37 °C with orbital shaking for 2 h. Then, 3-

chlorophenylhydrazone (CCCP; 10 μ L, 5 μ M) was added to one of the untreated bacterial suspensions as the depolarized control (positive control). Immediately after the addition of CCCP, the untreated, CCCP-treated, BiOI nanosheets-treated, and Au/BiOI nanocomposites-treated bacterial suspensions (1 mL) were incubated with DiOC₂ (10 μ L; 30 μ M) at room temperature for 30 min. Then, the mixtures were centrifuged (RCF 3,500 g, 10 min, 25 °C) and washed twice with PBS (pH 7.4, 1.0 mL \times 3) for measurement of bacterial membrane potentials, and for recording of fluorescence images of the stained bacteria using an Olympus IX71 microscope (Tokyo, Japan). The intensities of green fluorescence (excitation with blue light 460–480 nm) and red fluorescence (excitation with green light 510–530 nm) indicate the differences of membrane potentials in bacteria. The red/green ratios were calculated using mean fluorescence intensities of green and red fluorescence.

***In vitro* cytotoxicity tests.** The human embryonic kidney 293 cells (HEK-293T cells), murine fibroblast cell (NIH-3T3), human breast epithelial cells (MCF-10A), human umbilical vein endothelial cells (HUVEC) and rabbit corneal keratocytes (RCK cells) were obtained from American Type Culture Collection (ATCC, Manassas, VA, USA). The HEK-293T and RCK cells were maintained in DMEM medium; NIH3T3 in RPMI medium, and MCF-10A in alpha-MEM. Both medium were supplemented with FBS (10%), ampicillin (1%), L-glutamine (2.0 mM), and NEAA (1%) in 5% CO₂ at 37 °C. HUVECs were routinely cultured in tissue culture flasks in vasucLife® EnGS ECG medium in a 37 °C humidified atmosphere containing 95% air and 5% CO₂. In this study, all HUVECs were used between passages 2 and 5. The cell number was determined by the trypan blue exclusion method. Cell viability was determined using an MTT assay. Following the separate incubation of HEK-293T, NIH-3T3, MCF-10A, HUVEC and RCK cells (approximately 1.0 \times 10⁴ cells per well) in a culture medium for 72 h at 37 °C containing 5% CO₂, each of the culture media was replaced with 200 μ L of medium containing Au₁/BiOI nanocomposites of different concentrations (0–100 μ g mL⁻¹). The cells were then incubated for an additional 24 h. The cells were carefully rinsed thrice with PBS and treated with the MTT assay (10-fold dilution, 100 μ L per

well) for 4 h. Then, the absorbance at 570 nm was recorded using a Synergy 4 BioTek absorbance microplate reader. Since the absorbance is proportional to the number of metabolically active cells, the relative viability of cell cultures was calculated by assuming 100% viability in the Ctrl set (media without Au₁/BiOI nanocomposites).

Hemolysis assays. Hemolysis induced by BiOI nanosheets and Au₁/BiOI nanocomposites was tested according to a previous publication. Fresh blood samples from a healthy volunteer (Female, 25 years old) were drawn from the vein into tubes containing ethylenediaminetetraacetic acid (EDTA) and immediately (within 30 min of collection) centrifuged (RCF 3000 g, 10 min, 4 °C) to remove serum. The blood collecting procedures were performed in compliance with relevant laws and institutional guidelines. Fresh red blood cells (RBCs) were then washed thrice with sterile isotonic PBS. Following the last wash, the RBCs were diluted with sterile isotonic PBS to obtain an RBC stock suspension (8 vol % blood cells). The RBC stock suspension (250 μL, 8 % blood cells stock) was added to each BiOI nanosheets and Au₁/BiOI nanocomposites solution (250 μL with final concentration ranging from 0 to 100 μg mL⁻¹) in vials. After 1 h of incubation at 37 °C, each of the mixtures was centrifuged at RCF of 1000 g for 10 min. Hemolysis activity was determined by measuring hemoglobin absorption at 576 nm (OD₅₇₆) in the supernatant (200 μL). The sterile isotonic physiological buffer was used as a reference for 0% hemolysis (OD_{576 blank}). One hundred percent of hemolysis for the Ctrl was measured by adding ultrapure water to the RBC suspension (OD_{576 ultrapure water}). The hemolysis activity was calculated as follows:

$$\text{Hemolysis (\%)} = \frac{[(\text{OD}_{576 \text{ Au/BiOI}} - \text{OD}_{576 \text{ blank}})]}{(\text{OD}_{576 \text{ ultrapure water}} - \text{OD}_{576 \text{ blank}})} \times 100$$

Table S1. Atomic ratio analysis of BiOI nanosheets, Au_{0.1}/BiOI nanocomposites, Au₁/BiOI nanocomposites, and Au₁₀/BiOCl nanocomposites determined by elemental analysis and ICP-MS.

Nanomaterials	Bi (%)	Au (%)	O (%)	I (%)	Cl (%)
BiOI	27.8	n.d. ^a	28.2	44.0	n.d. ^a
Au_{0.1}/BiOI	39.1	0.40	40.7	19.8	n.d. ^a
Au₁/BiOI	32.5	6.20	35.7	23.8	1.80
Au₁₀/BiOCl	39.4	10.4	30.9	1.90	17.4

^anot detectable

Table S2. Comparison of the apparent Michaelis constants (K_M), maximal velocities (V_{max}), turnover number (K_{cat}), and catalytic efficiency (K_{cat}/K_M) of the BiOI nanosheets, Au_{0.1}/BiOI nanocomposites, Au₁/BiOI nanocomposites, and Au₁₀/BiOCl nanocomposites.

Nanomaterials	Substrate	K_M (nM) ^a	V_{max} (nM s ⁻¹) ^a	K_{cat} (nM·s ⁻¹ ·mL·μg ⁻¹) ^b	K_{cat}/K_M (s ⁻¹ ·mL·μg ⁻¹)
BiOI	AR	414	0.779	0.078	1.88×10^{-4}
Au_{0.1}/BiOI	AR	560	0.821	0.082	1.47×10^{-4}
Au₁/BiOI	AR	1009	4.32	0.432	4.28×10^{-4}
Au₁₀/BiOCl	AR	2115	2.92	0.292	1.38×10^{-4}

^aKinetic parameters of the nanomaterials (10 μg mL⁻¹) were determined according to the Lineweaver-Burk plot using the Michaelis–Menten Kinetic equation [$1/v = K_M/V_{max} \cdot (1/[S] + 1/K_M)$]; where v is the reaction velocity, $[S]$ is the substrate concentration, K_M is the Michaelis constant, and v_{max} is the maximal velocity. ^b $K_{cat} = V_{max}/[E]_{total}$, where $[E]_{total}$ is the concentration of nanomaterials (10 μg mL⁻¹).

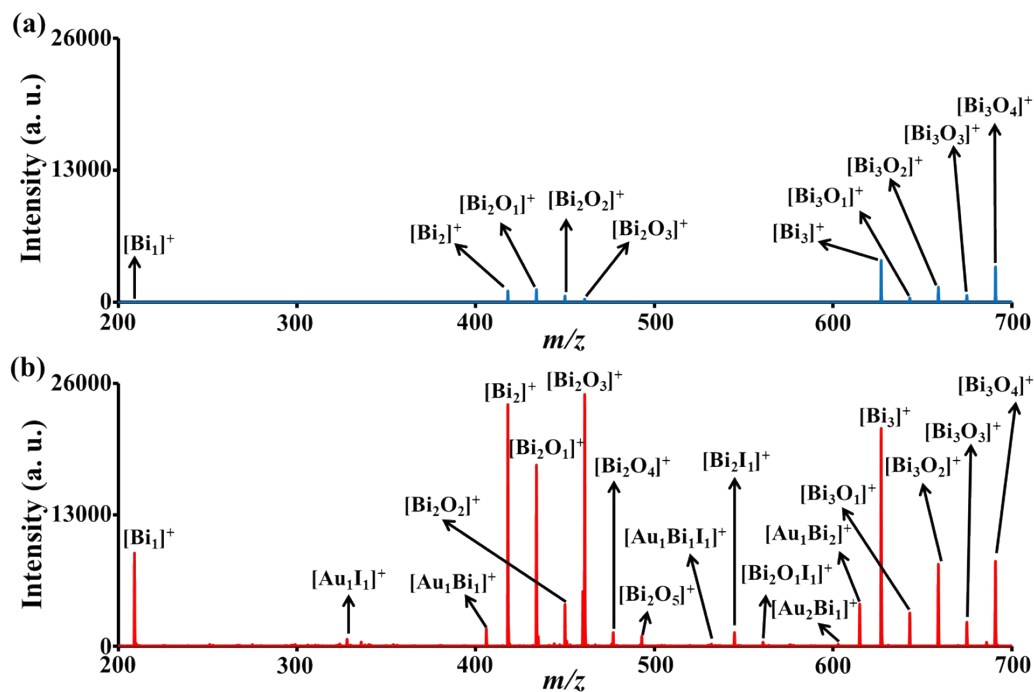


Figure S1. LDI-MS spectra of as-prepared (a) BiOI nanosheets and (b) Au₁/BiOI nanocomposites. The peaks at $m/z = 209.98, 324.88, 406.95, 418.97, 434.96, 450.96, 466.95, 482.95, 498.94, 533.86, 545.87, 561.87, 603.92, 615.93, 627.95, 643.94, 659.94, 675.93$ and 691.93 are assigned to [Bi₁]⁺, [Au₁I₁]⁺, [Au₁Bi₁]⁺, [Bi₂]⁺, [Bi₂O₁]⁺, [Bi₂O₂]⁺, [Bi₂O₃]⁺, [Bi₂O₄]⁺, [Bi₂O₅]⁺, [Au₁Bi₁I₁]⁺, [Bi₂I₁]⁺, [Bi₂O₁I₁]⁺, [Au₂Bi₁]⁺, [Au₁Bi₂]⁺, [Bi₃]⁺, [Bi₃O₁]⁺, [Bi₃O₂]⁺, [Bi₃O₃]⁺ and [Bi₃O₄]⁺ respectively. A total of 500 pulsed laser shots were applied to accumulate the signals from five LDI target positions under a laser power density of $5 \times 10^4 \text{ W cm}^{-2}$. Peak intensities are plotted in arbitrary units (a. u.).

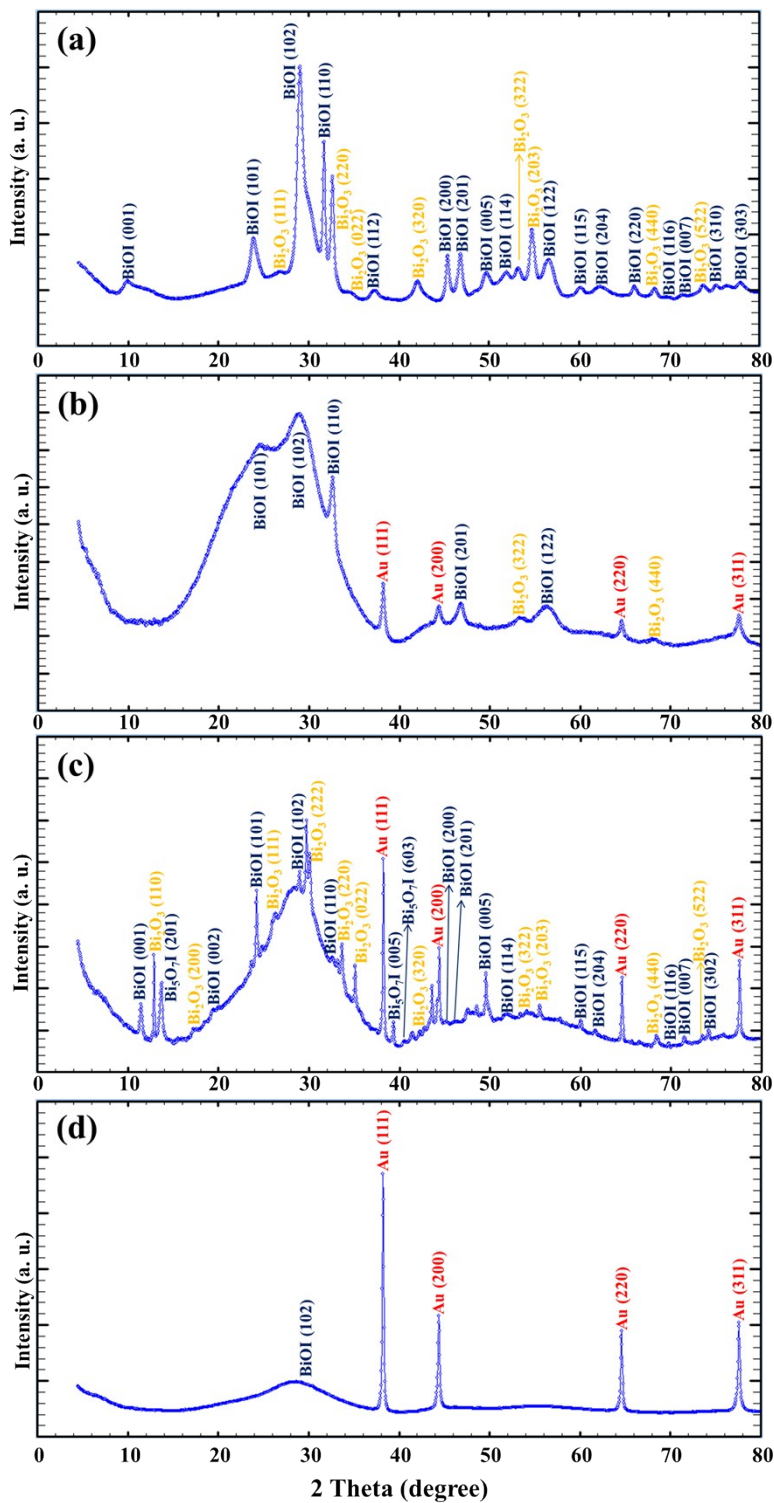


Figure S2. XRD patterns of (a) BiOI nanosheets, (b) Au_{0.1}/BiOI nanocomposites, (c) Au₁/BiOI nanocomposites, and (d) Au₁₀/BiOI nanocomposites. The XRD peaks of BiOI nanosheets or Au/BiOI nanocomposites are assigned corresponding to standard JCPDS 03-065-2870 (Au) and 10-0445 (BiOI; space group: *P4/nmm* (129), with lattice constants of *a* = 3.994 Å and *c* = 9.149 Å).

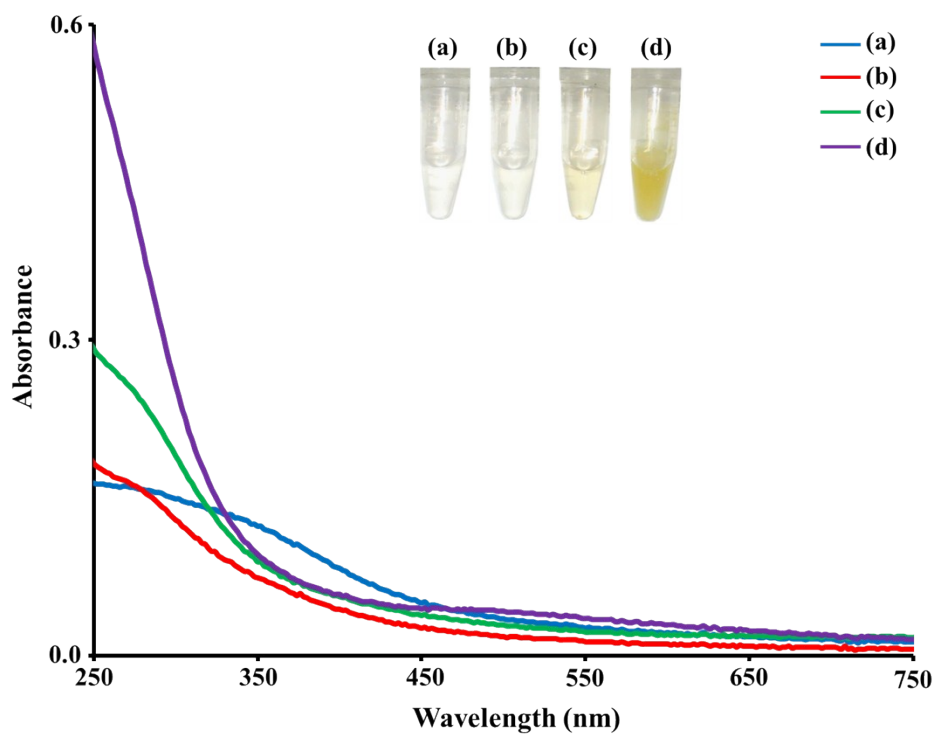


Figure S3. UV-Vis absorption spectra of (a) BiOI nanosheets, (b) Au_{0.1}/BiOI nanocomposites, (c) Au₁/BiOI nanocomposites, and (d) Au₁₀/BiOI nanocomposites in 5 mM Tris-borate (pH 7.0). The concentration of the nanosheet or nanocomposite particles was 20 $\mu\text{g mL}^{-1}$. The inset shows a photograph of the four corresponding solutions.

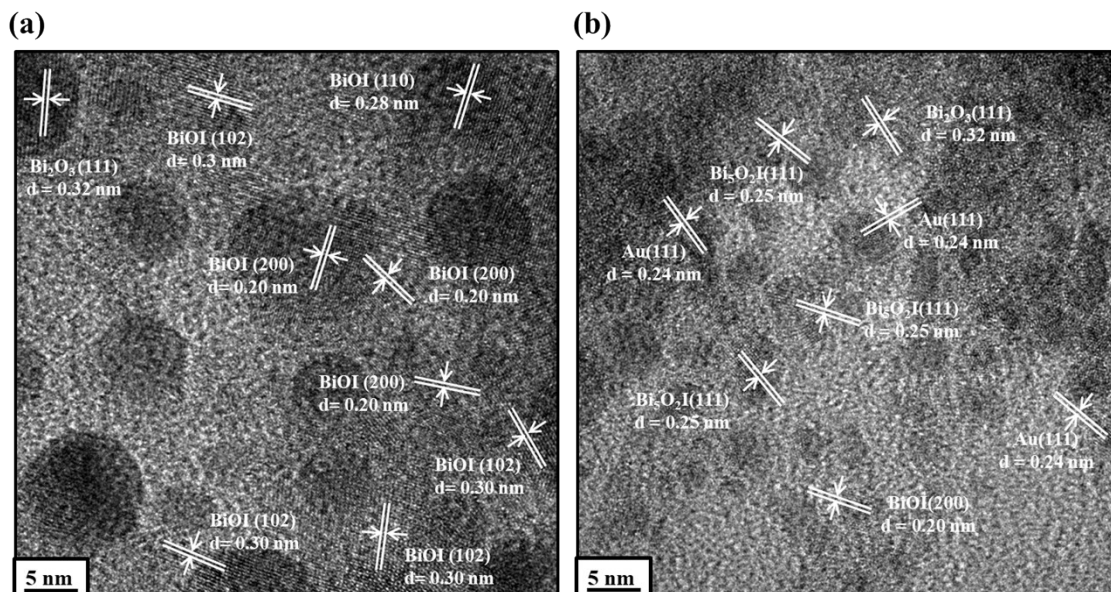


Figure S4. HRTEM images of (a) BiOI nanosheets and (b) Au₁/BiOI nanocomposites.

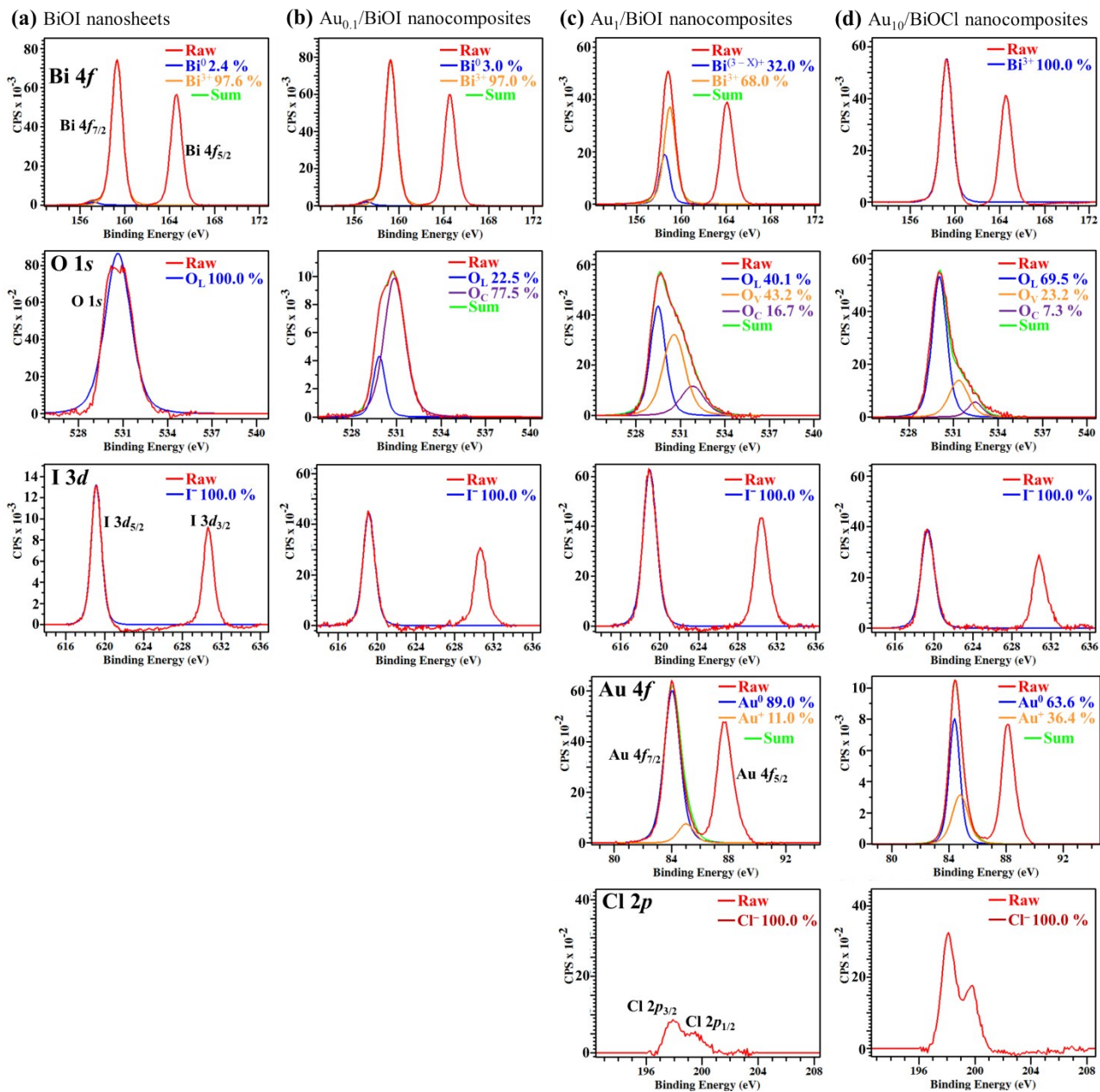


Figure S5. XPS spectra of as-prepared (a) BiOI nanosheets, (b) Au_{0.1}/BiOI nanocomposites, (c) Au₁/BiOI nanocomposites, and (d) Au₁₀/BiOCl nanocomposites.

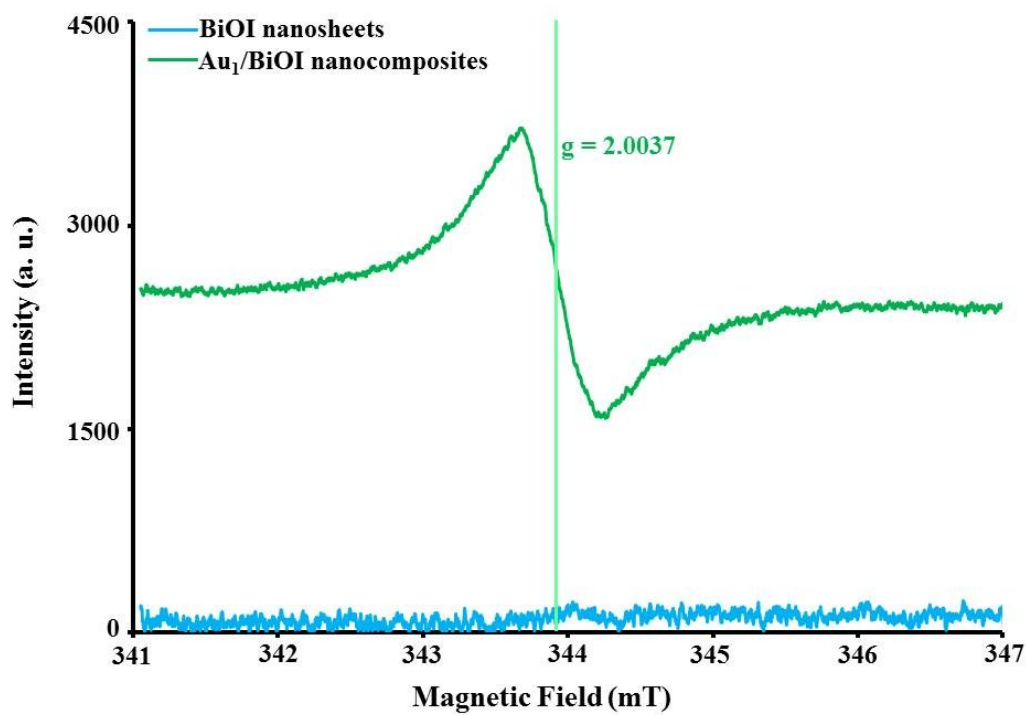


Figure S6. ESR spectra of BiOI nanosheets and Au₁/BiOI nanocomposites.

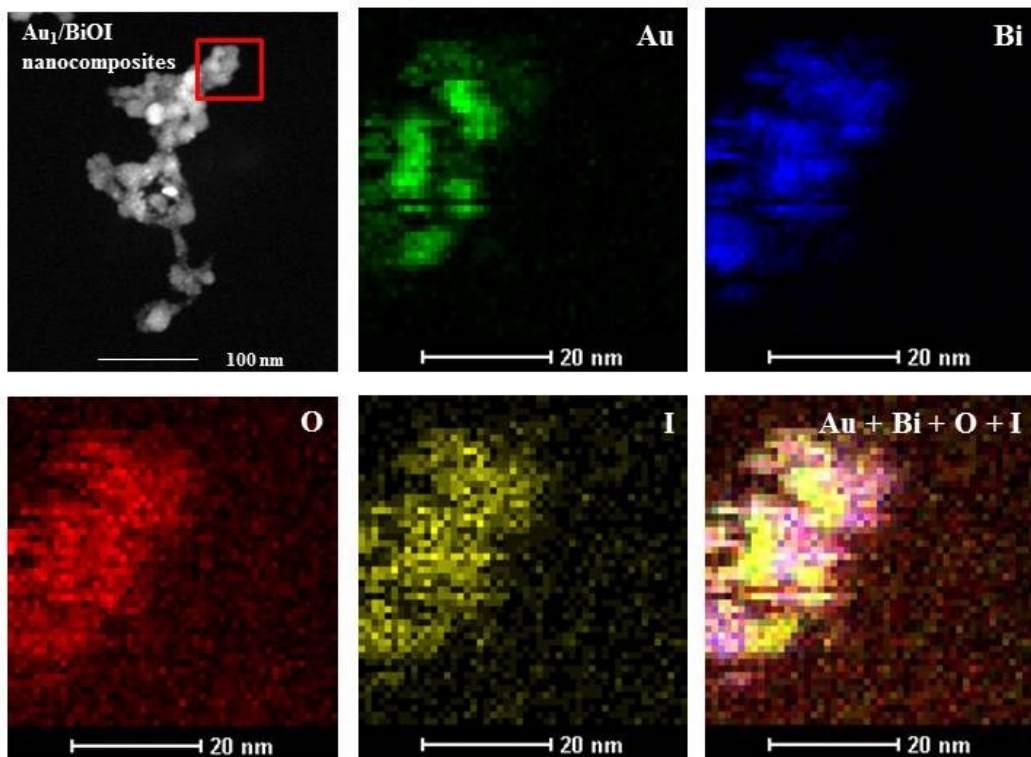


Figure S7. High-angle annular dark-field scanning TEM mapping images of Au₁/BiOI nanocomposites.

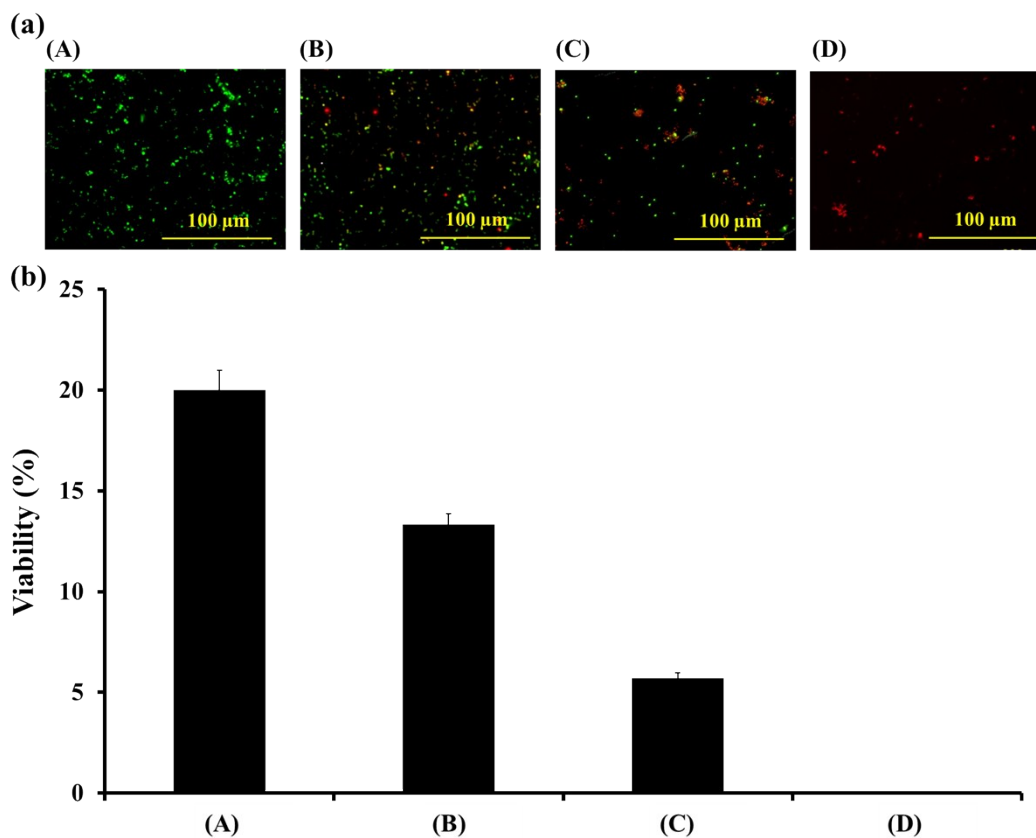


Figure S8. (a) Fluorescence images and (b) viability of *E. coli* (10^8 CFU mL⁻¹) in 5.0 mM sodium phosphate solution (pH 7.4) (A) untreated and (B–D) treated with Au₁/BiOI nanocomposites ($100 \mu\text{g mL}^{-1}$) for (B) 10, (C) 30, and (D) 60 min. Cells were stained with SYTO 9 and PI. Green fluorescent stains represent live cells, and red fluorescent stains represent dead or compromised cells. Error bars in (b) represent the standard deviation of three repeated measurements.

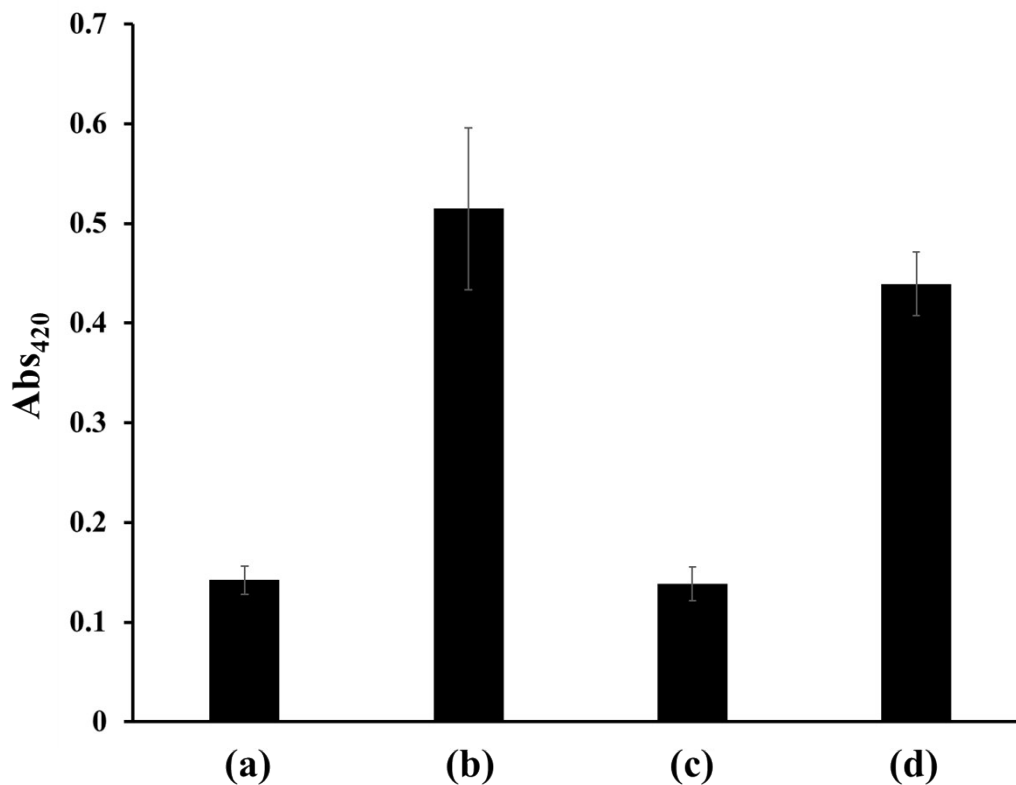


Figure S9. Absorbance of *o*-nitrophenol (ONP) at 420 nm (Abs_{420}) from the supernatants of *E. coli* (10^9 CFU mL⁻¹) solution (a) without and with (b–d) incubated (b) bacterial lysis solution (B-PER; as a Ctrl), (c) BiOI nanosheets ($100 \mu\text{g mL}^{-1}$), and (d) Au₁/BiOI nanocomposites ($100 \mu\text{g mL}^{-1}$). The reactions were carried out in 5.0 mM sodium phosphate solution (pH 7.4) containing 1.0 mM MgCl₂ and 10 mM KCl for 1 h. Error bars represented the standard deviation of three repeated measurements.

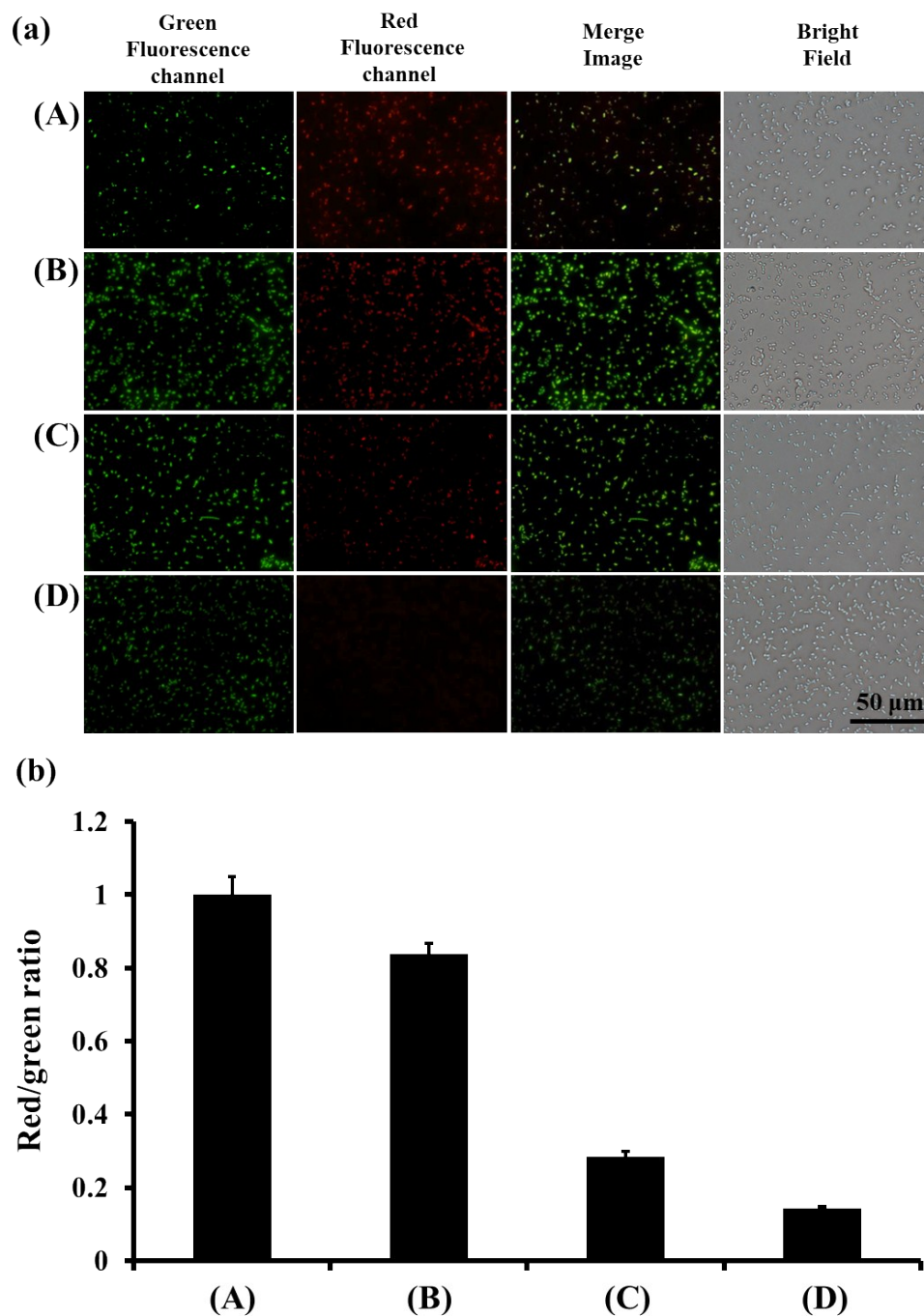


Figure S10. (a) Fluorescence images and (b) red/green cell ratio of (A) untreated and (B–D) treated *E. coli* (10^8 CFU mL⁻¹) with (B) BiOI nanosheets ($20 \mu\text{g mL}^{-1}$), (C) Au₁/BiOI ($20 \mu\text{g mL}^{-1}$), and (D) CCCP for 2 h. CCCP was used as positive control, which eliminates already built-up proton gradient across the membrane, and impairs the bacterial membrane potentials. The scale bar in (a) represents the size for each image. Error bars in (b) represented the standard deviation of three repeated measurements.

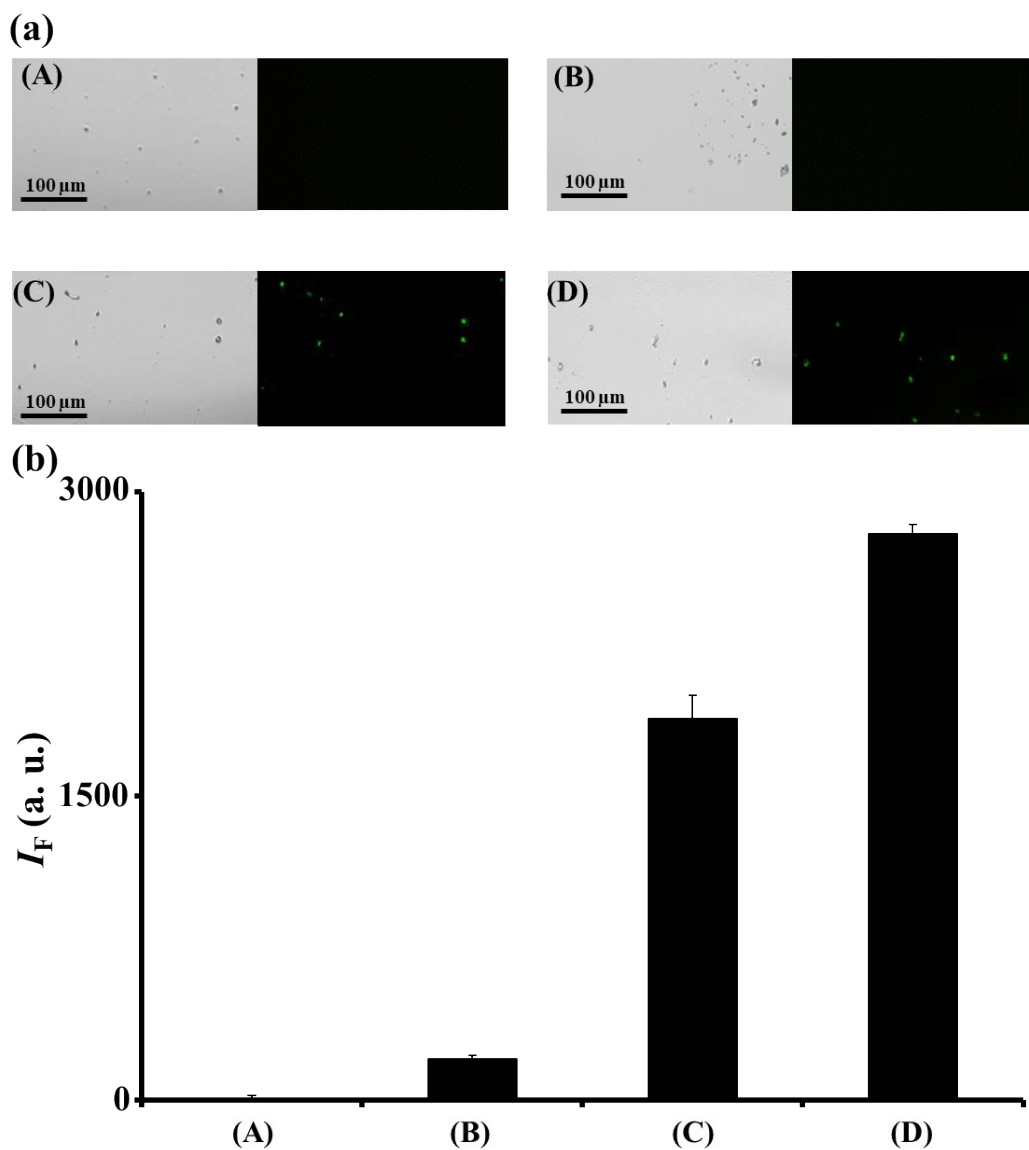


Figure S11. (a) Fluorescence images and (b) fluorescence intensities at 530 nm of *E. coli* (10^8 CFU mL^{-1}) in 5.0 mM sodium phosphate solution (pH 7.4) (A) untreated and (B–D) treated with (B) BiOI nanosheets ($20 \mu\text{g mL}^{-1}$), (C) Au_1/BiOI ($20 \mu\text{g mL}^{-1}$), and (D) H_2O_2 (1.0 mM) for 1 h. The fluorescence intensity (I_F) is plotted in arbitrary units (a. u.). Error bars represent the standard deviation of three repeated measurements.

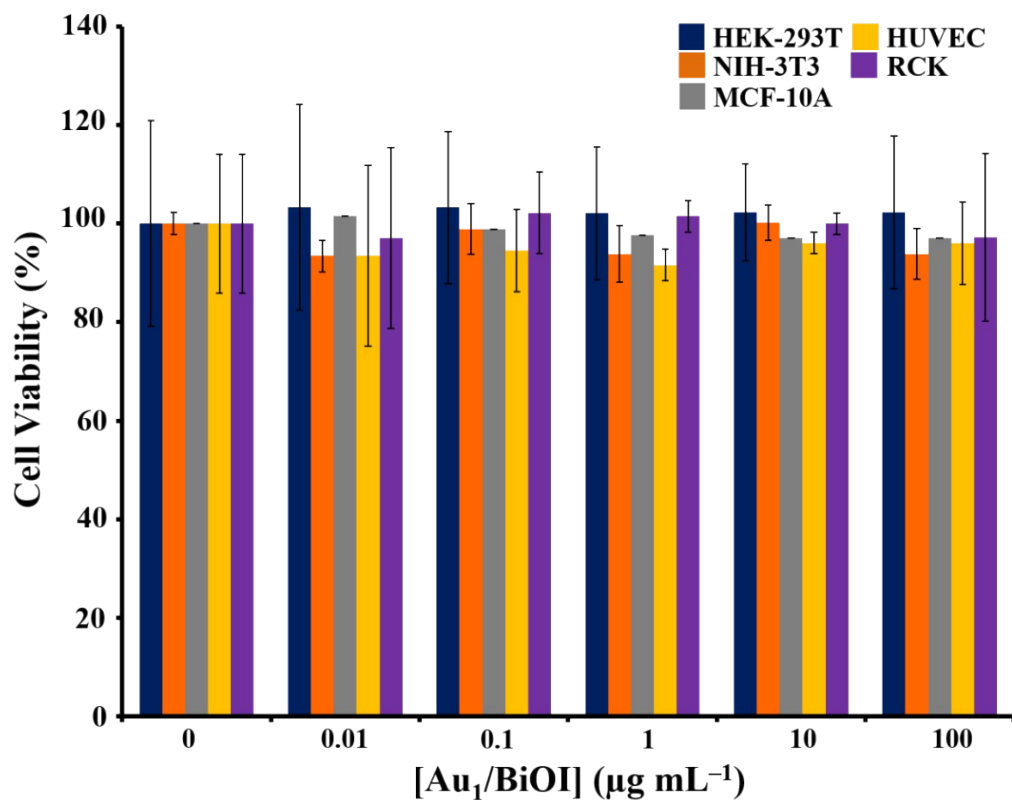


Figure S12. Viability of HEK-293T, NIH3T3, MCF-10A, HUVEC, and RCK cells (1.0×10^4 cells per well) after treatment with Au₁/BiOI nanocomposites (0–100 µg mL⁻¹) in culture media at 37 °C for 24 h. Error bars represent the standard deviation of three repeated measurements.

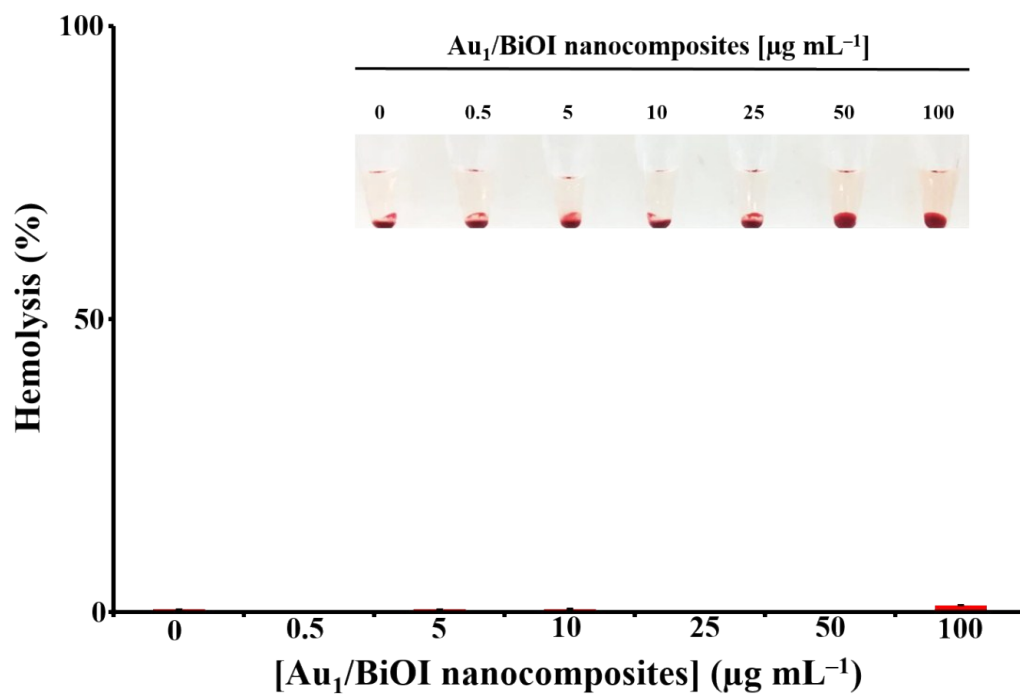


Figure S13. Hemolytic activities of Au₁/BiOI nanocomposites (0–100 µg mL⁻¹) solutions to RBCs. Inset: photographs of corresponding RBC solutions. Error bars represent the standard deviation of three repeated measurements.

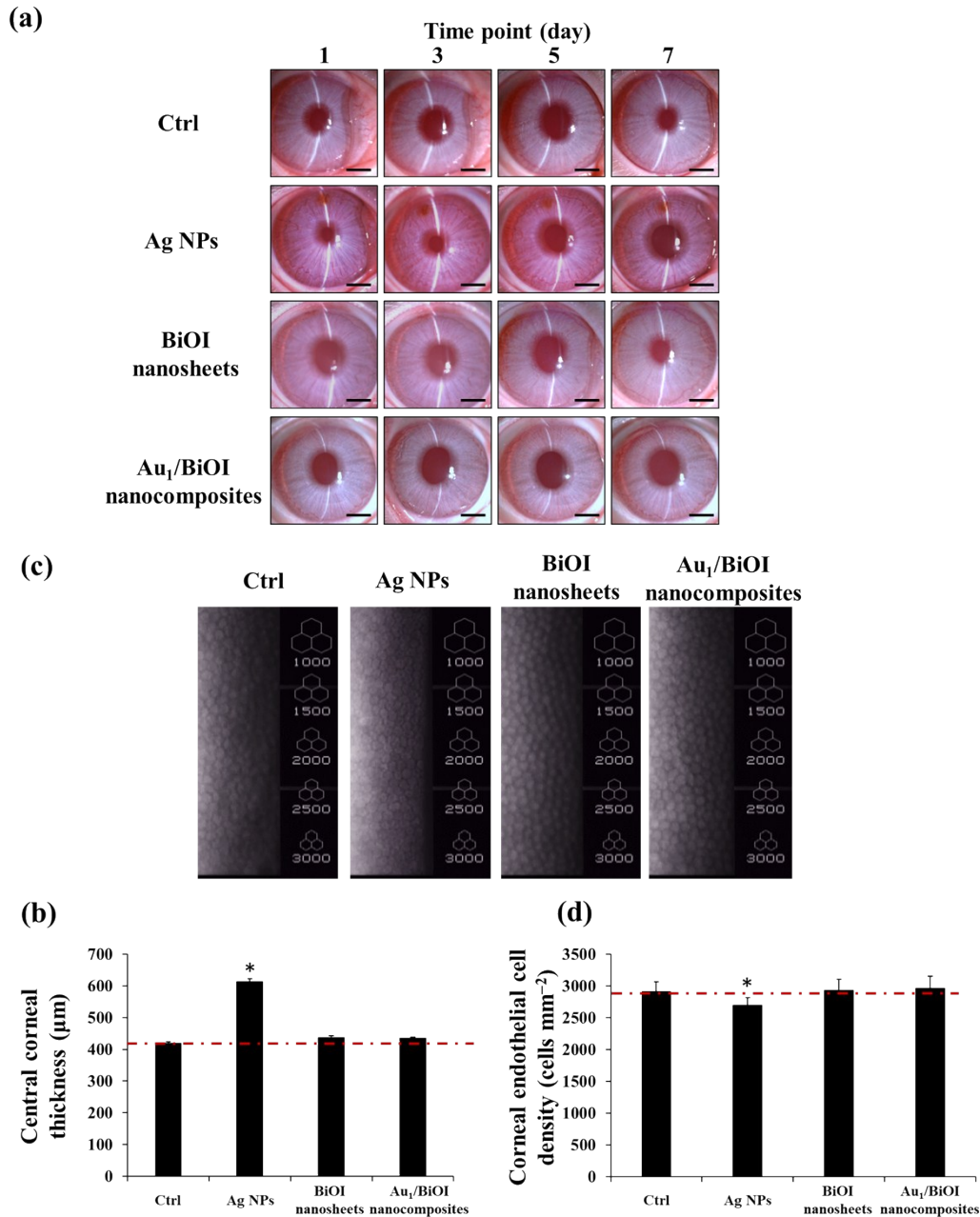


Figure S14. *In vivo* ocular biocompatibility of Ag NPs ($5 \mu\text{g mL}^{-1}$), BiOI nanosheets ($5 \mu\text{g mL}^{-1}$), and Au₁/BiOI nanocomposites ($5 \mu\text{g mL}^{-1}$) after intrastromal injection ($20 \mu\text{L}$) in rabbit eyes. The rabbits receiving PBS without nanomaterial serve as Ctrl group. (a) Time-course slit-lamp biomicroscopic images, (b–d) end-point (b) corneal thickness values, (c) specular microscopic images and (d) cell densities at 7 days postoperatively. Scale bars in (a): 5 mm. The red dash lines in (b) and (d) denote the preoperative values for corneal thickness and endothelial cell density, respectively. Asterisks indicate statistically significant differences ($*p < 0.05$; $n = 6$) as compared with the Ctrl groups.